Journal of Alloys and Compounds 509 (2011) 3602–3605

Contents lists available at ScienceDirect

Journal of Alloys and Compounds

journal homepage: www.elsevier.com/locate/jallcom

Synthesis of Ti_3SiC_2 bulks by infiltration method

Di Shan[a,b], Guo Yan[b,*], Lian Zhou[a,b], Chengshan Li[b], Jinshan Li[a], Guoqing Liu[b], Jianqing Feng[b]

[a] The State Key Laboratory of Solidification Processing, Northwestern Polytechnical University, Xi'an 710072, China
[b] Northwest Institute for Nonferrous Metal Research, Xi'an 710016, China

ARTICLE INFO

Article history:
Received 31 August 2010
Received in revised form
24 November 2010
Accepted 14 December 2010
Available online 22 December 2010

Keywords:
Infiltration
Ti_3SiC_2 bulks
Reaction mechanism

ABSTRACT

T_3SiC_2 bulks have been synthesized by infiltrating Si liquid into porous precursor pellets composed of solid TiC and Ti powders. Silicon pellets were placed at the bottom of the precursor pellets as the liquid source. The starting compositions can be represented by the formula $2TiC + Ti + xSi$, where $x = 1.0$, 1.2, 1.5 and 1.8, respectively. The phase formation and microstructure of the bulks were investigated by X-ray diffraction (XRD) and scanning electron microscopy (SEM) equipped with energy-dispersive spectroscopy (EDS) system. The results demonstrated that the TiC/Ti precursor pellet could only react with Si completely when the x value is 1.8. Impurities SiC, Ti–Si binary compounds and Ti_8C_5 appeared along the silicon diffusion direction. It is found that the compositions of impurities strongly depended on the Si-concentration. Reaction mechanism of this Ti_3SiC_2 infiltration synthesis has also been discussed based on the Si-concentration changes on the diffusion path.

1. Introduction

Ti_3SiC_2 ternary compound exhibits the characteristics of both ceramic and metal [1], such as high electrical and thermal conductivities, unusually damage tolerance, extremely low coefficient of friction with μ less than 0.005 on cleavage faces along the basal plane [2], and excellent oxidation resistance at elevated temperature up to 1273 K [3]. All these features make Ti_3SiC_2 an excellent candidate for many practical applications as bearings, turbine blades, drills, pantograph slider plates, and corrosive protective coatings.

However, so far there is still no mature technology to fabricate large bulks of Ti_3SiC_2. It has been reported that the infiltration method is an effective way in fabricating large single grain Y–Ba–Cu–O superconductors [4,5]. We think that Ti_3SiC_2 bulks with not only high density and purity, but also large dimensional parameters could be prepared with the infiltration method. As an initial phase of the study, only the feasibility of Ti_3SiC_2 bulks synthesis has been investigated. Although Lim et al. reported that with the precursor pellet made of TiC, high-purity Ti_3SiC_2 phase could be synthesized since Ti_3SiC_2 with the infiltration method between TiC and Si melt seemed to be directly synthesized without forming intermediate phases such as $TiSi_2$ and Ti_5SiC_x [6], it is not clear for the effects of Si-concentration changes on the phase evolution along the Si diffusion direction. Generally speaking, lack of Si will cause the incompletion of reactions and residual TiC and Ti phase, while excess of Si will lead to the appearance of Ti–Si secondary phase. So the starting Si ratio must be an important parameter in the infiltration process.

In the present study, Ti_3SiC_2 bulks have been synthesized by the infiltration method at 1773 K with the starting materials of TiC, Ti, and different ratios of Si. The possible reaction mechanism of Ti_3SiC_2 fabricated by the process has also been discussed.

2. Experimental

The powders of TiC (99% in purity, 40–45 μm in average size) and Ti (99%, 40–45 μm) were weighted in a molar ratio of TiC:Ti = 2:1, and grinded for half an hour in the air to guarantee the uniformity. The mixture was pressed under the pressure of 10 MPa into $\phi = 30$ mm pellets with 6.5% aqueous solution of poly vinyl alcohol (PVA) as both the adhesive and pore-forming agent. The function of the pore-forming agent is to dehydrate at high temperature to make the TiC/Ti precursor pellets porous, which can greatly improve the capillary action of liquid silicon. Then the precursor pellets were heated at 673 K for 1 h under Ar atmosphere for the PVA dehydration.

The Si powder (99%, 40–45 μm) was weighted according to the formula $2TiC + Ti + xSi$, where $x = 1.0$ (S1), 1.2 (S2), 1.5 (S3) and 1.8 (S4), respectively. The silicon pellets also with the diameter of 30 mm were prepared under the pressure of 10 MPa without PVA and then placed under the precursor pellets. The schematic illustration of this infiltration process was presented in Fig. 1. These samples were placed in alumina crucibles and heated in vacuum furnace. They were firstly heated to 1273 K at the heating rate of 1200 K h^{-1}, then to 1773 K at 300 K h^{-1}, and held at this temperature for 3 h, finally furnace-cooled to room temperature.

In order to investigate the phase evolution with the Si-concentration changes on the diffusion path, the pellets were cut along the direction perpendicular to the top surface into two identical pieces, and the Ti_3SiC_2 region on both S2 and S4 have been cut into five sections (named as (a)–(e), respectively) in equal thickness from bottom to top.

The phase composition was identified by X-ray diffraction (XRD, Philips PW 1710) with Cu Kα radiation. The morphology was observed by scanning electron

* Corresponding author. Tel.: +86 29 86231079; fax: +86 29 86224487.
E-mail address: gyan@c-nin.com (G. Yan).

0925-8388/$ – see front matter © 2010 Elsevier B.V. All rights reserved.
doi:10.1016/j.jallcom.2010.12.092

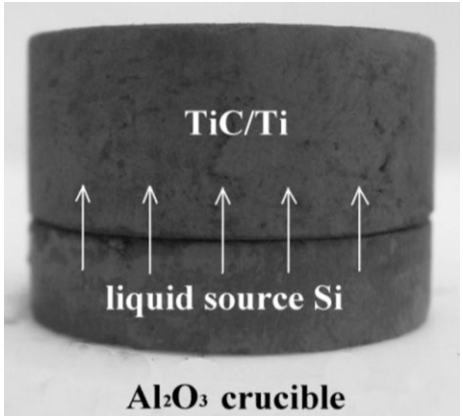

Fig. 1. Schematic illustration of the infiltration process applied in this study.

microscopy (SEM, Model JSM-6460). The elemental analysis was carried out with an energy-dispersive spectroscopy (EDS).

3. Results

Fig. 2(a) and (b) shows the amplificatory images of S2 ($x = 1.2$) and S4 ($x = 1.8$), respectively. The overall vertical-section of S2 can be obviously divided into two different parts. The upper region is mainly composed of Ti_8C_5 and the lower one is of fully reacted Ti_3SiC_2. In S4, no obvious boundary can be observed, representing for the only Ti_3SiC_2 region, which means the $x = 1.8$ is appropriate for the infiltration synthesis of Ti_3SiC_2. Moreover, the morphologies of S1 and S3 are similar as that of S2, in all of which the Ti_8C_5 can be observed due to the lack of Si source.

Fig. 3 exhibits the XRD patterns taken from the vertical-sections of S1–S4. In S1–S3, the diffraction peaks of Ti_8C_5 are stronger than that of Ti_3SiC_2 due to the large amount of the residual TiC/Ti. Besides Ti_8C_5, a small quantity of Ti–Si binary compounds and SiC were also detected. The optimized result was obtained in S4 with the major phase of Ti_3SiC_2. It can be concluded that higher silicon content than stoichiometry is necessary for the synthesis of Ti_3SiC_2, and the optimized value of x should be ~1.8.

Fig. 4 presents the XRD patterns of the five sections from S2. It can be noticed that Ti_3SiC_2 is formed as the major phase in the reacted region. Along the silicon diffusion direction, it can be observed that: SiC appears and no other impurity can be detected in section (a); the impurity changes into Ti_5Si_3 in section (b); in addition to Ti_5Si_3, $TiSi_2$ and SiC can also be identified in section (c)

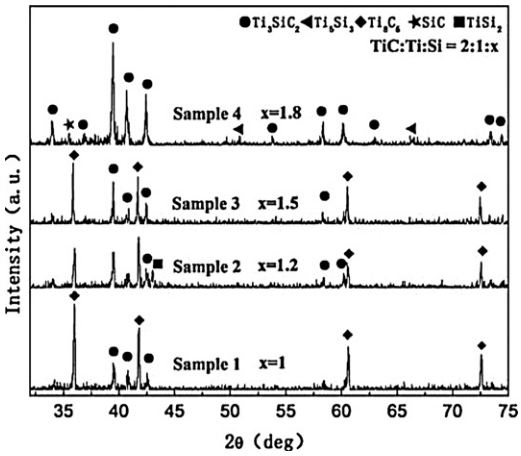

Fig. 3. XRD patterns of the vertical-sections of S1–S4 after heating at 1773 K for 3 h in vacuum.

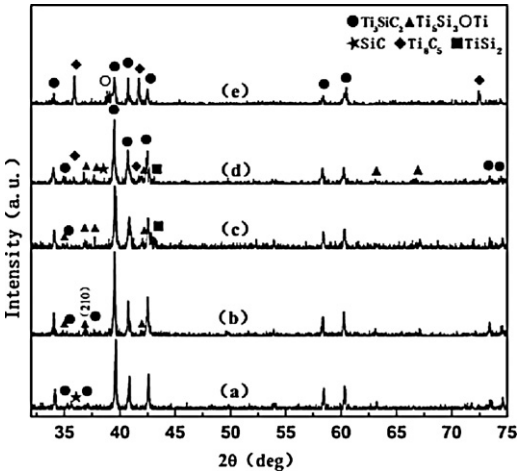

Fig. 4. XRD patterns of the cross-sections of S2 along the silicon diffusion direction.

and (d); the impurities can be indexed into Ti_8C_5 and Ti in section (e). So it can be concluded that along the Si diffusion path, the composition of these impurities tended to change from Si–C and Ti–Si into Ti–C compounds.

Fig. 5 presents the XRD patterns of the five sections (a)–(e) from S4. Ti_8C_5 still can be detected on the top surface, shown on pattern (e). It is noteworthy that with the addition of a large excess of

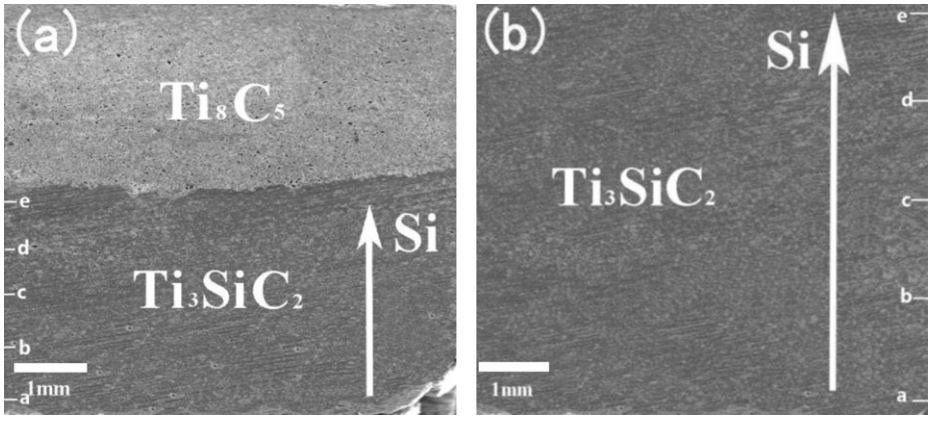

Fig. 2. Microstructures of the vertical-sections of sintered bulks. The gray area is the porous Ti_8C_5 region and the dark area is the dense Ti_3SiC_2 region. (a) S2 ($x = 1.2$), (b) S4 ($x = 1.8$).

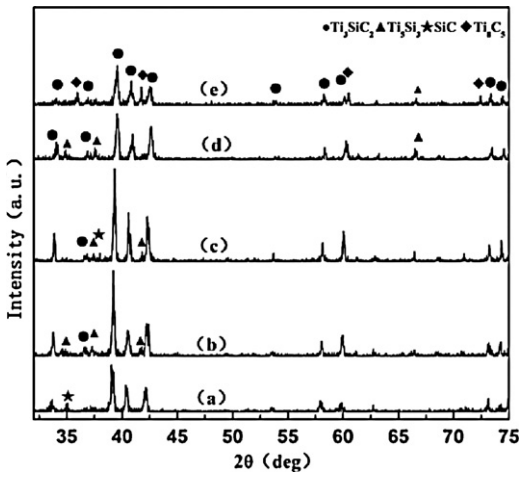

Fig. 5. XRD patterns of the cross-sections of S4 along the silicon diffusion direction.

silicon, the purity of Ti_3SiC_2 in S4 has been greatly improved compared with S2. The (2 1 0) peak of Ti_5Si_3 ($2\theta = 36.74^\circ$) in Fig. 4 can be obviously detected, but it, as well as the $TiSi_2$ peaks, disappears in Fig. 5.

The SEM images of S2 were shown in Fig. 6(a) and (b). These grains exhibit an equiaxial feature with homogenous particle size. Fig. 6(b) displays an obvious boundary which divides the bulk into two different parts: the left part is the porous Ti_8C_5 region; the right part is the dense Ti_3SiC_2 region. Fig. 6(c) and (d) illustrates the microstructures of S4 with a layered structure. The apparent density has been measured as 4.38 g cm^{-3}. Compared the microstructures of S2, the grains in S4 are apparently larger, which indicates that the average particle size becomes larger with the increase of the silicon.

In Fig. 7(a) and (b), the atomic ratio of Ti:Si:C of S4 has been analyzed by EDS. In order to obtain the atomic ratio of Ti/Si/C, one part which was cut along the direction perpendicular to the top surface was placed on the test-bed, which can move with the step length of 0.5 mm in the thickness direction. The scanning area of each step is 200 μm × 250 μm. Normalized results are shown in Fig. 7(a). The values of Ti/Si/C atomic ratio are also measured when

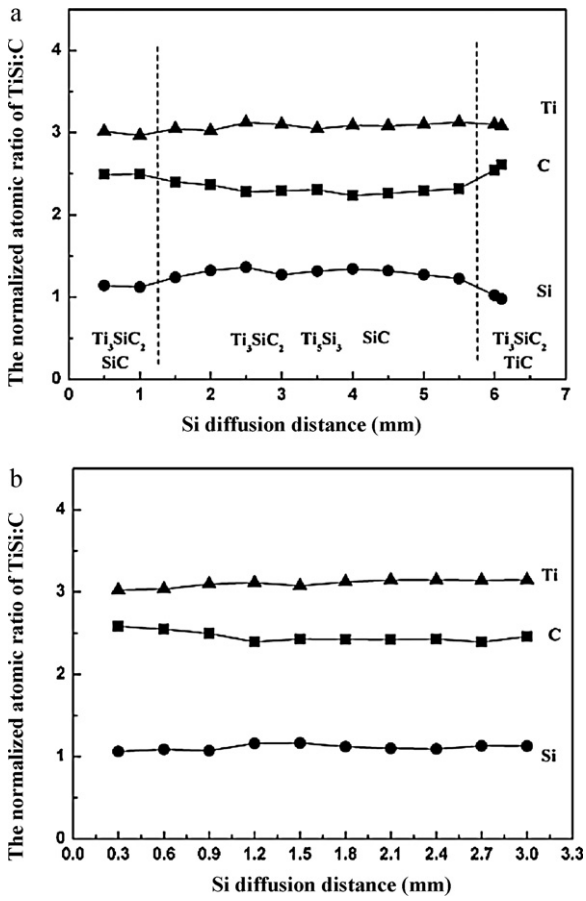

Fig. 7. The normalized atomic ratio of Ti:Si:C of S4 analyzed by EDS. (a) measured in the thickness direction with the step length of 0.5 mm (b) measured in the diameter direction with the step length of 0.3 mm.

the test-bed moved in the diameter direction with the step length of 0.3 mm, as shown in Fig. 7(b). In both directions, only slight composition fluctuation can be observed due to the appearance of impurities.

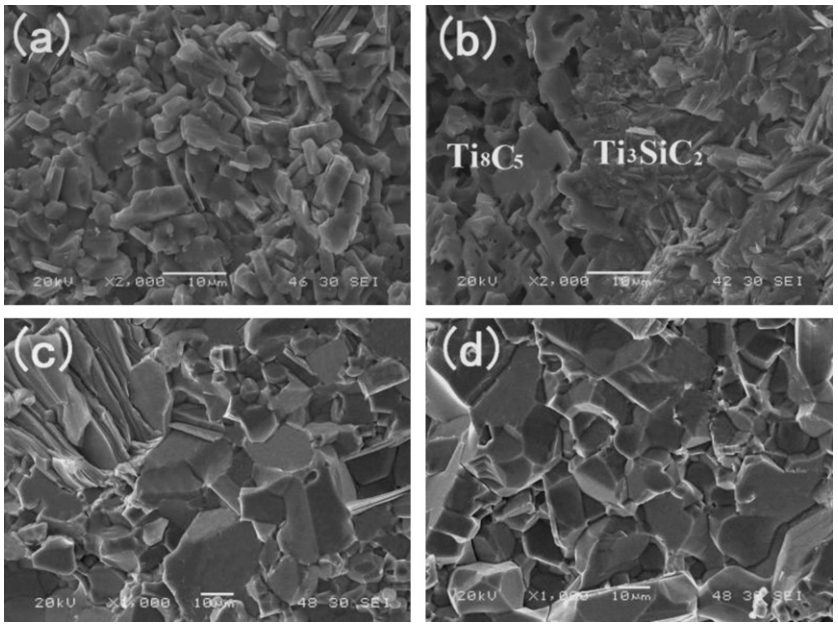

Fig. 6. SEM images of the samples along the silicon diffusion direction. (a) and (b) S2, (c) and (d) S4.

4. Discussion

Although the reaction mechanism of Ti_3SiC_2 fabricated by other methods have been previously reported [1,7–9], in our infiltration synthesis study, there is an obviously different feature has been found during the phase formation process, which is that the phase compositions are closely related to the Si-concentration changes along the diffusion path. So we will discuss about the reaction mechanism of infiltration preparation of Ti_3SiC_2.

At the bottom of the Ti_3SiC_2 region, the atomic ratio of Ti:Si is close to 3:1.1, as shown in Fig. 7(a). SiC as the only impurity was detected. The existence of SiC should be described as follow [10]:

$$3TiC + 2Si \rightarrow Ti_3SiC_2 + SiC \quad (1)$$

After the formation of SiC, Ti, TiC and SiC were involved into a new reaction to form Ti_3SiC_2 [11]:

$$2Ti + TiC + SiC \rightarrow Ti_3SiC_2 \quad (2)$$

The solid-state diffusion in reaction (2) is a slow process, so there will be a certain amount of SiC left, due to the rapid consumption of Ti and TiC in another solid–liquid reaction, which will be given in the next part.

In the middle part of the Ti_3SiC_2 region, the average atomic ratio of Ti:Si is about 3:1.3. Taking the XRD results in Figs. 4(b)–(d) and 5(b)–(d) into account, the Ti–Si binary compounds and a small amount of SiC were detected together with Ti_3SiC_2. According to the Ti–Si binary phase diagram, there are two eutectic phases as Ti_5Si_3 and $TiSi_2$ at 1606 K [12], as well as several other Ti–Si compounds. The compositions of precipitated Ti–Si compounds are strongly dependent on the starting Ti:Si ratio. In some previous study, with the starting Ti:Si ratio of 5:3, Ti_5Si_3, Ti_5Si_4, TiSi and $TiSi_2$ were detected in the resultants. After the Ti:Si ratio change to 1:2, the resultants were consisted of $TiSi_2$ with a small amount of Si and Ti_5Si_3 [13]. Sun et al. concluded that the appearance of $TiSi_2$ can be contributed to the excess of silicon [14]. In our experiment, we think that the formation of $TiSi_2$ is dependent on the localized Si-concentration. During the infiltration processes, the driving force can be recognized as the resultant force of the upward capillary force, the downward viscous resistance and gravity. So after the infiltrating of Si into the middle part of precursor bulk, the resistance results in the decrease of Si diffusion rate, the accumulated silicon in the local area lead to the formation of $TiSi_2$. The liquid sources (both the melted silicon and Ti–Si binary compounds) react with the solid particles and form Ti_3SiC_2 as shown below:

$$Ti - Si\,(l) + TiC_x \rightarrow Ti_3SiC_2 \quad (0.625 \leq x \leq 1) \quad (3)$$

Differential scanning calorimeter (DSC) analysis has been carried out on the identical mixture of TiC and Ti as the precursor pellet with the same heating parameters. From the result, we think that the stable phase Ti_8C_5 was synthesized during the dwell time. It implies that x in TiC_x are of the values from 0.625 to 1 during the formation of Ti_3SiC_2.

From reaction (3), it can be noticed that if Ti–Si binary compounds are residual in the resultants, there should also be TiC_x. However, from the XRD profiles, Ti_5Si_3 can always be detected as impurity, but no obvious TiC_x phase can be identified in this region. So the total consumption of TiC_x should not only due to the reaction (3), but also the reaction (1). This conclusion can be testified by a small quantity of SiC residual.

On the interface between the Ti_8C_5 region and the reacted Ti_3SiC_2 region (S2) or on the top surface of the bulk (S4), the atomic ratio between Ti and Si is about 3:1. From the XRD analysis in Figs. 4(e) and 5(e), Ti_8C_5/Ti appeared and Ti–Si compounds completely disappeared. Although the liquid source diffused into the precursor pellet completely (S4), it is the evaporation of silicon made the Ti_8C_5 remain on the top surface.

In this experiment, a large amount of Si is used, but single phase Si has not been found from all the XRD patterns. Except for the Ti–Si compounds and SiC, the excess Si should be evaporated during the heating. According to the thermodynamic data, the vapor pressure of Si is 5×10^{-1} Pa at 1773 K [15], which is two orders of magnitude higher than the pressure in our vacuum system ($\sim 10^{-3}$ Pa). During the heat treatment, it was observed that the pressure in vacuum furnace rise from $\sim 10^{-3}$ Pa to $\sim 10^{0}$ Pa, which can be considered as the evidence of Si vaporization. On the other hand, it should be pointed out that the final Ti:C ratio is 3:(2.25–2.5) obtained from Fig. 7, while the starting Ti:C ratio is only 3:2. The excess C should be caused by the decomposition of PVA.

From aforementioned results, it is found that different impurities appeared with the change of the Si-concentration. It is possible that the optimization of the proportion of original powders is a promising way to synthesize the Ti_3SiC_2 bulk with higher density and purity, as well as larger dimensional parameters.

5. Conclusions

The initial materials with a large excess of silicon, 2TiC/Ti/1.8Si, are necessary to obtain the high-pure Ti_3SiC_2 bulk with the infiltration method. The reaction mechanism of Ti_3SiC_2 changes with the Si-concentration changes on the Si diffusion path. At the bottom of the Ti_3SiC_2 region with Ti:Si ≈ 3:1.1, the impurity is mainly SiC. In the middle part of the Ti_3SiC_2 region with Ti:Si ≈ 3:1.3, Ti–Si compounds and a little of SiC are detected. On the top of the Ti_3SiC_2 region with Ti:Si ≈ 3:1, the Ti_8C_5/Ti are identified.

Acknowledgements

This work was supported by the National Natural Science Foundation of China (no.50672077) and National Basic Research Program of China (no.2011CBA00104).

References

[1] M.W. Barsoum, T. El-Raghy, J Am. Ceram. Soc. 79 (1996) 1953–1956.
[2] S. Myhra, J.W.B. Summers, E.H. Kisi, Mater. Lett. 39 (1999) 6–11.
[3] M.W. Barsoum, T. El-Raghy, Am. Sci. 89 (2001) 336–343.
[4] Y.L. Chen, H.M. Chan, M.P. Harmer, V.R. Todt, S. Sengupta, D. Shi, Phys. C 234 (1994) 232–236.
[5] K. Iida, N. Hari Babu, Y. Shi, D.A. Cardwell, Supercond. Sci. Technol. 18 (2005) 1421–1427.
[6] B. Lim, S.W. Park, S.S. Lee, T.W. Kim, Ceram. Eng. Sci. Proc. 22 (2001) 89–95.
[7] J.F. Li, F. Sato, R. Watanabe, J. Mater. Sci. Lett. 18 (1999) 1595–1597.
[8] Y. Zou, Z.M. Sun, S. Tada, H. Hashimoto, J. Alloys Compd. 441 (2007) 192–196.
[9] J.M. Córdoba, M.J. Sayagués, M.D. Alcalá, F.J. Gotor, J. Am. Ceram. Soc. 90 (2007) 825–828.
[10] S.S. Hwang, S.W. Park, T.W. Kim, J. Alloys Compd. 392 (2005) 285–290.
[11] Z.F. Zhang, Z.M. Sun, H. Hashimoto, T. Abe, Scripta Mater. 45 (2001) 1461–1467.
[12] J.T. Li, Y. Miyamoto, J. Mater. Synth. 7 (1999) 91–96.
[13] H. Hashimoto, Z.M. Sun, Y.L. Du, W.B. Tian, J. Alloys Compd. 484 (2009) 483–488.
[14] Z.M. Sun, S. Yang, H. Hashimoto, Ceram. Int. 30 (2004) 1873–1877.
[15] J.C.S. Pires, J. Otubo, A.F.B. Braga, P.R. Mei, J. Mater. Process. Tech. 169 (2005) 16–20.